Experimental evaluation of plasticity-induced crack shielding from crack tip displacements fields

J.M. Vasco-Olmo, F.A. Díaz
University of Jaén, Departamento de Ingeniería Mecánica y Minera, Campus Las Lagunillas, Edificio A3, 23071, Jaén, Spain
jvasco@ujaen.es, fdiaz@ujaen.es

ABSTRACT. In this work it is proposed a methodology for the evaluation of plasticity-induced crack shielding from the analysis of the crack tip displacements fields measured by digital image correlation. This methodology is based on the evaluation of the stress intensity factors determined from the displacements fields measured at the vicinity of the tip of a growing fatigue crack. For the characterisation of the crack tip displacements field, CJP model has been implemented. This model considers the shielding effects due to plasticity generated during fatigue crack growth. For the purpose of the current work, several fatigue experiments at different *R*-ratios have been conducted on Al2024-T3 compact tension specimens. In addition, compliance based methods have been adopted to perform a comparison of the results with those obtained by DIC. Results show a good level of agreement, illustrating the enormous potential of DIC technique for the study of fracture mechanics problems.

KEYWORDS. Plasticity-induced crack shielding; Fatigue; Stress intensity factor; Digital image correlation.

INTRODUCTION

Fatigue crack growth generates a plastic zone at the crack tip and along the crack flanks, which may induce plasticity-induced crack closure [1]. This phenomenon is one of the crack tip shielding mechanisms that reduces the stress intensity factor range originated at the crack tip. However, there are still some issues that remain unresolved or misunderstood regarding crack closure, which are mainly associated with problems in its measurement and interpretation [2].

Recently, the use of digital image correlation (DIC) has become very popular for the analysis of structural integrity problems. Thus, different methodologies based on the calculation of stress intensity factors (SIFs) from the displacement fields measured around a tip of growing cracks have been developed [3 – 6]. In particular, the method developed by James et al. (CJP model) [6] which takes into account the effect of plasticity generated around the crack tip during fatigue growth. Thus, it considers an analysis of the shielding effect over the surrounding elastic field.

In the current work, it has been performed an experimental evaluation of plasticity-induced crack shielding from the displacements fields measured at the vicinity of the crack tip using DIC. Thus, CJP model [6] has been implemented for the characterisation of the crack tip displacements fields. Moreover, for the purpose of this work, fatigue tests at different *R*-ratios on Al2014-T3 CT (compact-tension) specimens have been conducted. Results have been compared with those obtained using the strain offset calculation, showing a good level of agreement which highlights the potential of DIC to evaluate the shielding effect during fatigue crack growth.

FUNDAMENTALS OF THE MODEL FOR CHARACTERISING CRACK TIP DISPLACEMENTS FIELDS

JP model is a novel mathematical methodology developed by Christopher, James and Patterson [6] based on Muskhelishvili's complex potentials [7] which considers that the plastic enclave that exists around a fatigue crack tip and along the crack flanks will shield the crack from the full influence of the applied elastic stress fields. Crack tip shielding includes the effect of crack flank contact forces and a compatibility-induced interfacial shear stress at the elastic-plastic boundary. Fig. 1 illustrates schematically the forces acting at the interface of the plastic zone and the surrounding elastic field material. F_{Ax} and F_{Ay} are the reaction forces to the applied remote load. This load generates the T-stress and the corresponding force F_T. The above forces cause a plastic zone at the crack tip, deforming permanently the material and inducing the forces F_{Px} and F_{Py} during unloading. F_S is the induced force by the interfacial shear at the elastic-plastic boundary of the crack wake. F_C is the force generated when the plastic wakes contact during unloading, so the crack closes under the action of the elastic field.
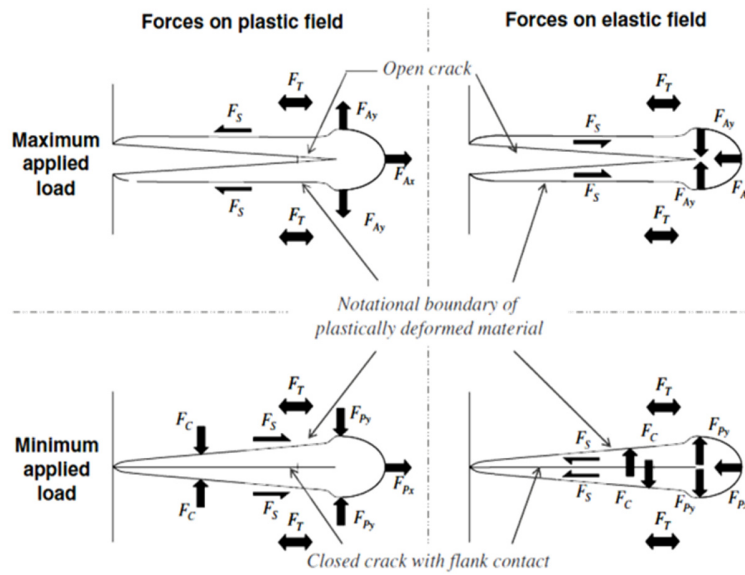

Figure 1: Schematic idealisation of the forces acting at the elastic-plastic boundary [6].

According to this model, the crack tip displacements field can be described as follows:

$$2G(u+iv) = \kappa \left[-2(B+2E)z^{\frac{1}{2}} + 4z^{\frac{1}{2}} - 2Ez^{\frac{1}{2}}\ln z - \frac{C-F}{4}z \right]$$
$$- z\left[-(B+2E)\overline{z}^{-\frac{1}{2}} - E\overline{z}^{-\frac{1}{2}}\overline{\ln z} - \frac{C-F}{4} \right] \qquad (1)$$
$$- \left(A\overline{z}^{\frac{1}{2}} + D\overline{z}^{\frac{1}{2}}\overline{\ln z} - 2D\overline{z}^{\frac{1}{2}} + \frac{C+F}{4}\overline{z} \right)$$

Where $G = \dfrac{Y}{2(1+v)}$ is the shear modulus, Y and v are the Young's modulus and the Poisson's ratio of the material respectively, $\kappa = \dfrac{3-v}{1+v}$ for plane stress or $\kappa = 3-4v$ for plane strain, z is the complex coordinate and A, B, C, D, E and F are unknown coefficients.

Thus, this new model employs four parameters to characterise the stress and displacement fields around the crack tip generated by the forces as indicated in Fig. 1. Where K_F is an opening mode stress intensity factor, K_R a retardation stress intensity factor, K_S shear stress intensity factor and T the T-stress.

K_F is characterised by the driving crack growth force F_A generated by the remote load:

$$K_F = \sqrt{\frac{\pi}{2}}\left(A - 3B - 8E\right) \tag{2}$$

K_R is characterised by F_C and F_P that induce a shielding effect on the crack tip and therefore a retardation effect of fatigue crack growth:

$$K_R = \frac{\pi^{3/2}}{\sqrt{2}}\left(D - 3E\right) \tag{3}$$

K_S is characterised by F_S that acts in the interfacial boundary between the generated plastic zone and the surrounding elastic field:

$$K_S = \sqrt{\frac{\pi}{2}}\left(A + B\right) \tag{4}$$

Finally, the T-stress is characterised by F_T generated by the remote load:

$$T_x = -C; \quad T_y = -F \tag{5}$$

EXPERIMENTAL PROCEDURE

The main objective of the current work is the experimental evaluation of the retardation effect on fatigue crack growth. For this purpose, two fatigue tests at different *R*-ratios on CT Al2024-T3 specimens (Fig. 2a) were conducted. The first test was conducted at low *R*-ratio ($R = 0$), while the second one was at high *R*-ratio ($R = 0.5$). Thus, a loading cycle between 5 and 600 N was used for the first test, and between 600 and 1200 N for the second one. Both tests were conducted at a cycling frequency of 10 Hz employing a 100 kN MTS 370.10 servohydraulic machine (Fig. 2b).
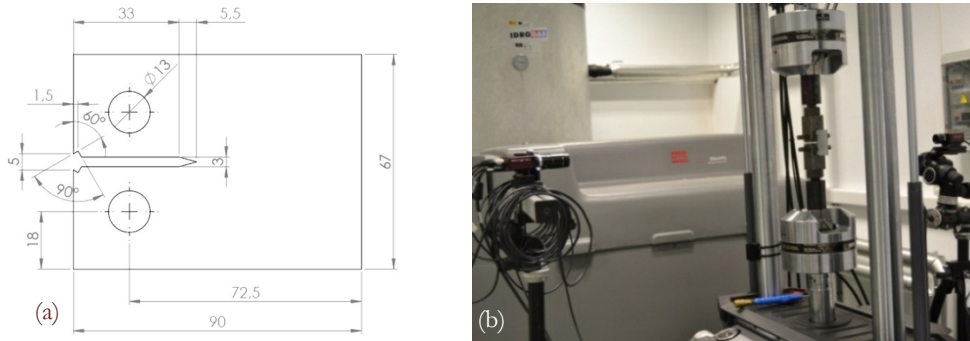

Figure 2: CT specimen (a) and experimental set-up (b) used for fatigue testing.

As it was indicated above, the retardation effect was evaluated from the analysis of the SIFs calculated from the displacements field measured around the crack tip using 2D-DIC. Thus, for the implementation of the technique a sequence of images was captured with a monochromatic CCD camera (Allied Vision Technologies, model Stingray F-504B/C) placed perpendicularly to the specimen surface with a 75 mm lens controlled by an E6510 IntelCore i5 Dell-Latitude laptop with the aid of a FWB-EC3402 video. In addition, the specimen surface was prepared to obtain a random speckle pattern by spraying it with black paint over a previously painted white background. In addition, an extra camera (Allied Vision Technologies, model Pike F-032B/C) was located at the back of the specimen to track the crack tip and monitor the crack growth during fatigue experiments.

Moreover, results from DIC were compared with those obtained from the implementation of strain offset technique. Thus, the opening and closing loads were estimated from the analysis of crack opening displacement (COD) data collected from an MTS 632.03F-30 extensometer with a data sampling of 5 Hz.

EXPERIMENTAL METHODOLOGY FOR SIF CALCULATION

In this work, the evaluation of plasticity-induced crack shielding was made from the analysis of the SIFs calculated from the displacements fields measured around the crack tip. Hence, the development of an experimental methodology to calculate SIFs was essential. The first step in the methodology was capturing a sequence of images during fatigue experiments from a reference state (undeformed) until a deformed state at different loading steps. After capturing the sequence of images and before its processing, the areas corresponding to the notch and the grips were masked since these areas did not add any relevant information. The next was the image processing, for this task the commercial software package Vic-2D [8] was employed. As an example, Fig. 3 shows the displacements fields measured for a 34.10 mm crack at a load of 600 N.
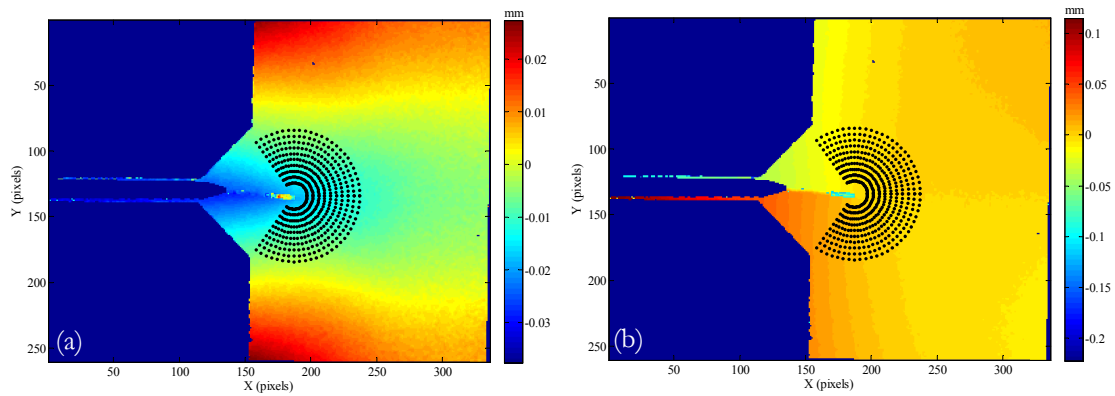

Figure 3: Horizontal (a) and vertical (b) displacement fields measured for a 34.10 mm and a load level of 600 N.

According to Eq. 1, the relationship between the displacements and the unknown coefficients is linear. Therefore SIFs can be obtained solving a system of linear equations. Thus, an error function was defined to relate the experimental data (displacement fields) with a mathematical expression according to the model. It is important to indicate that rigid body motion was considered in the formulation (horizontal and vertical translation, and rotation), otherwise the adopted DIC algorithm would consider it as a virtual displacement induced by the applied load. Finally, experimental SIFs have been compared with those nominal values predicted by ASTM E647-99 [10] according to the following expression:

$$\Delta K_{nom} = \frac{\Delta P}{t\sqrt{W}} \frac{2 + \frac{a}{W}}{\left(1 - \frac{a}{W}\right)^{\frac{3}{2}}} \left[0.886 + 4.64\frac{a}{W} - 13.32\left(\frac{a}{W}\right)^2 + 14.72\left(\frac{a}{W}\right)^3 - 5.6\left(\frac{a}{W}\right)^4 \right] \qquad (6)$$

Where ΔP is the loading range, t and W are the thickness and the width of the specimen, respectively, and a is the crack length.

EXPERIMENTAL RESULTS AND DISCUSSION

In this section, experimental results obtained from the analysis of the displacement fields measured on the specimens tested are presented and discussed.

Fig. 4 shows the experimental K_F and K_R values along the loading cycle for a specimen tested at low R-ratio at a crack length of 34.10 mm. In addition, nominal K_I values according to Eq. 6 have been also presented. From the analysis of K_F, it is observed that from a load level of 150 N, the experimental values agree with the nominal values. However, below the load level above indicated K_F values are higher than K_I values. It is observed a gradual change in the trend followed by K_F values as the load decreases. This behaviour is similar to that reported by Elber when defining plasticity-induced crack closure phenomenon. He noticed an anomaly in the elastic compliance of several fatigue specimens. Thus, he argued that this change in compliance was due to the contact between crack surfaces at low load levels higher than zero. According to this, opening (K_{op}) and closing (K_{cl}) stress intensity factors can be estimated from K_F trend as that value corresponding to

the minimum applied load (red line in Fig. 4) for the loading and unloading branch respectively. Moreover, from the analysis of K_R, a sign change is observed as the load reaches 100 N. Thus, below this load K_R takes positive values, while above this load K_R changes its sign. Therefore, it can be established that K_R values divide the loading cycle in two portions, thus the first portion corresponds to the loading interval at which the crack is closed, while the second portion corresponds to the interval at which the crack is open. According to this, there is a correspondence between the change in the K_F trend and the sign change in K_R.
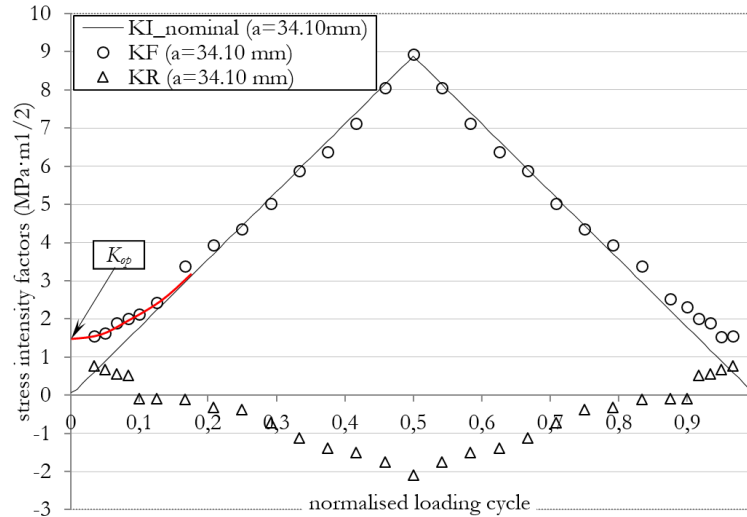

Figure 4: SIFs obtained for the specimen tested at low *R*-ratio corresponding to a crack length of 34.10 mm

The adopted methodology can be extrapolated to estimate K_{op} and K_{cl} as a function of the crack length. In Fig. 5, estimated K_{op} and K_{cl} values at the different analysed crack lengths for the specimen tested at low *R*-ratio have been plotted. It can be observed a gradual increase of K_{op} and K_{cl} values along the crack length. These are above K_{min} and hence, it highlights that the crack opens or closes at a load higher than the minimum applied load. In addition, it can be observed that there are not big differences between K_{op} and K_{cl} values.

Moreover, crack opening (P_{op}) and closing (P_{cl}) loads can be calculated from K_{op} and K_{cl} values previously estimated using Eq. 6. Thus, results have been plotted in Fig. 6 together with the minimum and maximum loads of the applied loading range. It is observed that as the crack grows P_{op} and P_{cl} values are within a load range (75 N ≤ P_{op}, P_{cl} ≤ 125 N) which corresponds to a percentage of 12.5 and 21 % of the maximum applied load. Nevertheless, some scatter is observed which can be attributed to the fact that crack opens or closes in a gradual way, and consequently, it is difficult to establish a single value for P_{op} or P_{cl}. Thus, there is an interval at which crack changes from fully closed to fully open.

Once DIC results have been analysed, results from the strain offset calculation are exposed and discussed. The signal collected from the extensometer was divided into two data sets corresponding to the loading and unloading branches of the applied load. In addition, the COD signal was filtered to minimise the influence of noise. For the implementation on the method, the two branches are represented on a load versus COD plot, and a least-squares straight line is fit to experimental data at the part of the loading cycle at which the crack is fully open. For this purpose, a segment that spanned a range of approximately 25 % of the loading cycle range is selected to represent a fully open crack configuration. Then, a linear fit corresponding to the load range to fully open crack is employed to calculate the theoretical COD for a particular load value. The difference between theoretical and experimental COD values is calculated to obtain the strain offset. Finally, the strain offset is presented as a function of the applied load, and P_{op} from the loading branch and P_{cl} from the unloading one are obtained as the load value at which the strain offset reaches the zero value.

Fig. 7 shows the results obtained from strain offset method for a 35.47 mm crack corresponding to the specimen tested at low R-ratio. Plots located on the left correspond to results for the loading branch, while those located on the right correspond to the unloading branch. Top plots show the applied load versus the measured COD for loading (left) and unloading (right) branches. In both plots, it can be observed raw data, filtered data and a fitted line corresponding to no closure. This line has been obtained considering data results above 150 N (corresponding to a 25 % of the load range) and performing a least squares fitting.
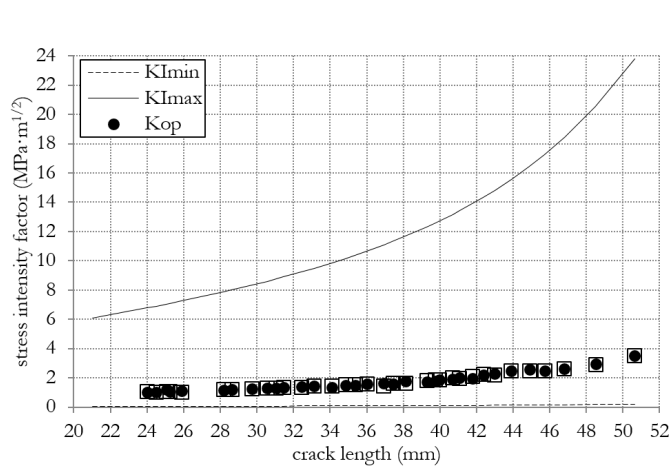
Figure 5: Estimated K_{op} and K_{cl} values as a function of the crack length for the specimen tested at low *R*-ratio.
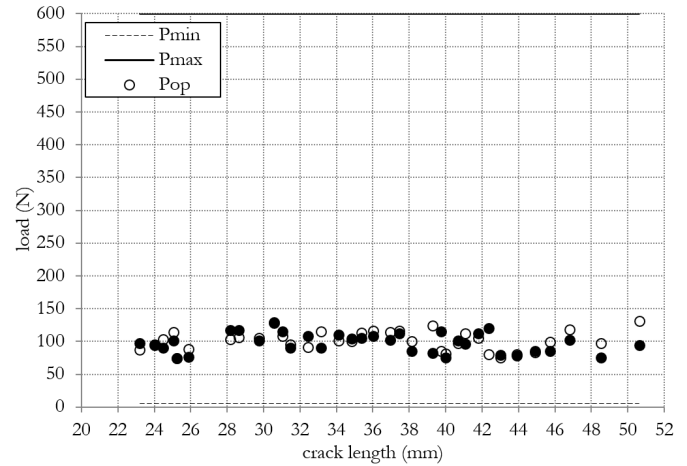
Figure 6: P_{op} and P_{cl} at different crack lengths for the specimen tested at low *R*-ratio.

From top plots, it can be observed a change in the slope of experimental data for load values between 100 and 110 N, which indicates that crack starts opening. However, from bottom plots, it is observed that for load values higher than 100 N (for loading branch) and 115 N (for unloading branch) the strain offset is almost 0, which indicates that the crack is completely open. According to this, P_{op} and P_{cl} values can be estimated for all the analysed crack lengths (Fig. 8). In Fig. 8 it can be observed that P_{op} and P_{cl} values are between 75 N and 125 N, with no apparent differences between P_{op} and P_{cl} values. Therefore, these results show great level of agreement with those obtained from CJP model, so the experimental methodology proposed to estimate P_{op} and P_{cl} values from K_F trend can be considered as validated.
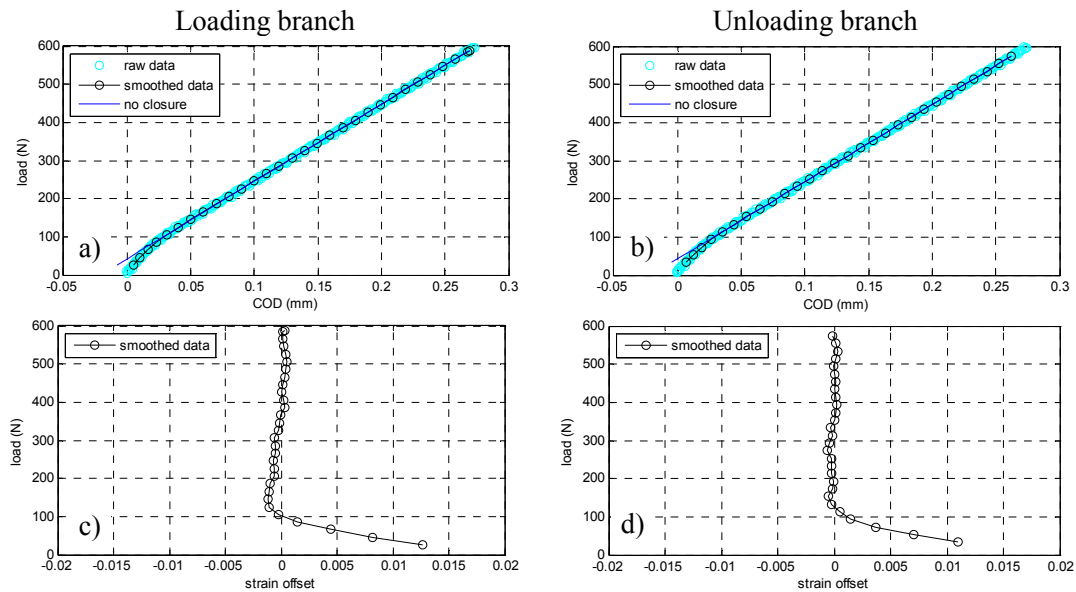

Figure 7: Results obtained from strain offset method for a crack length of 35.47 mm corresponding to the specimen tested at low *R*-ratio. a) Applied load versus COD for loading branch, b) applied load versus COD for unloading branch, c) applied load versus strain offset for loading branch and d) applied load versus strain offset for unloading branch.

In a similar way, results from the specimen tested at high *R*-ratio have been also analysed. K_F and K_R values obtained as a function of the loading cycle at crack lengths of 34.64 and 41.09 mm are shown in Fig. 9. It is observed that K_F values show total level of agreement throughout the whole loading cycle with those calculated from Eq. 6. Therefore, there is no change in the slope of K_F as in the case of the specimen tested at low *R*-ratio, which indicates the absence of the shielding effect and consequently, the crack remains fully open during the loading cycle. In addition, this behaviour is also observed

from the analysis of K_R, where there is no change in its sign during the loading cycle, which is interpreted as no variation in crack configuration and therefore, the crack keeps fully open throughout loading cycle.
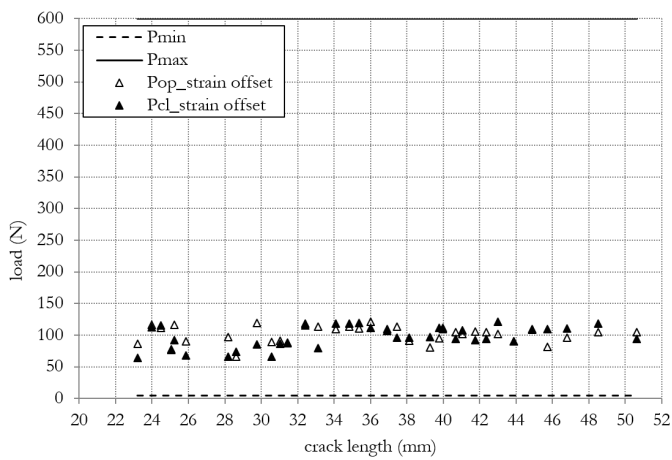

Figure 8: P_{op} and P_{cl} values obtained at different crack lengths for the specimen tested at low R-ratio using the strain offset method.
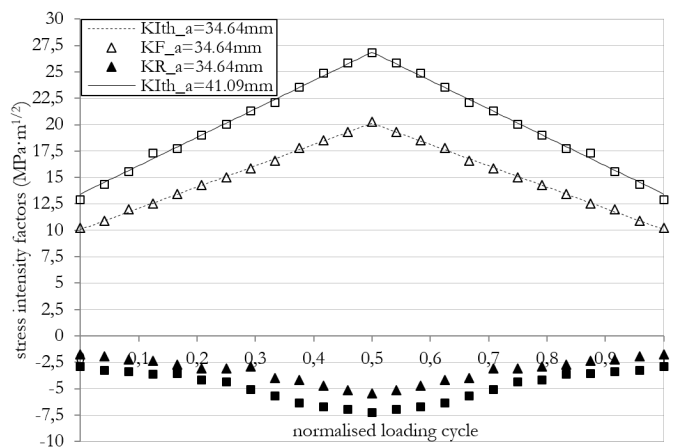
Figure 9: Experimental K_F and K_R corresponding to the specimen tested at high R-ratio for two different crack lengths (34.64 and 41.09 mm).

CONCLUSIONS

Digital image correlation has been employed to evaluate plasticity-induced crack shielding from the analysis of the stress intensity factors defined in CJP model and calculated from the measured crack tip displacement fields on Al-2024 CT specimens. An experimental methodology to estimate P_{op} and P_{cl} values has been proposed, being based on the analysis of K_F trends for the loading and unloading branches respectively. Shielding effect during fatigue crack growth has been observed in the specimen tested at low R-ratio. However, this phenomenon has not been observed for the specimen tested at high R-ratio. Results from DIC have been compared with those obtained from a compliance based method, showing a good level of agreement and illustrating the potential that both DIC technique and CJP model present to evaluate the plasticity-induced crack shielding effect and consequently, fracture mechanics problems.

REFERENCES

[1] Elber, W., Fatigue crack closure under cyclic tension, Eng. Fract. Mech., 2, 1 (1970) 37-45.
[2] James, M.N., Some unresolved issues with fatigue crack closure measurement, mechanisms and interpretation problems, Advance in Fracture Research, Proceedings of the ninth International Conference on Fracture. Edited by B.L. Karihaloo et al., Pergamon Press, 5 (1996) 2403-14.
[3] Ewalds, H.L., Wanhill, R.J.H., Fracture Mechanics, Edward Arnold, London, UK (1991).
[4] Yates, J.R., Zanganeh, M., Tai, Y.H., Quantifying crack tip displacement fields with DIC, Eng. Fract. Mech., 77 (2010) 2063-76.
[5] López-Crespo, P., Sheterenlikht, A., Patterson, E.A., Withers, P.J., Yates, J.R., The stress intensity factors of mixed mode cracks determined by digital image correlation, J. Strain Anal. Eng. Design, 43 (2008) 769-80.
[6] James, M.N., Christopher, C.J., Lu, Y., Patterson, E.A., Local crack plasticity and its influences on the global elastic stress field, Int. J. Fatigue, 46 (2013) 4-15.
[7] Muskhelishvili, N.I., Some Basic Problems of the Mathematical Theory of Elasticity, Noordhoff International Publishing, Groningen, Netherlands (1977).
[8] http://www.correlatedsolutions.com/vic-2d/
[9] Sanford, R.J., Dally, J.W., A general method for determining the mixed-mode stress intensity factors from isochromatic fringe pattern, Eng. Fract. Mech., 11 (1979) 621-33.
[10] E647-99, Standard test method for measurement of fatigue crack growth rates. Philadelphia: American Society for Testing and Materials (1999).

[11] Elber, W., Fatigue crack closure under cyclic tension, Eng. Fract. Mech., 2, 1 (1970) 37-45.

[12] Skorupa, M., Beretta, S., Carboni, M., Machniewicz, T., An algorithm for evaluating fatigue crack closure from compliance measurements, Fatigue Fract. Eng. Mater. Struct., 25 (2002) 261-73.